



HAL
open science

Mutations on VEEV nsP1 relate RNA capping efficiency to ribavirin susceptibility

Nadia Rabah, Oney Ortega Granda, Gilles Quérat, Bruno Canard, Etienne Decroly, Bruno Coutard

► To cite this version:

Nadia Rabah, Oney Ortega Granda, Gilles Quérat, Bruno Canard, Etienne Decroly, et al.. Mutations on VEEV nsP1 relate RNA capping efficiency to ribavirin susceptibility. *Antiviral Research*, 2020, 182, pp.104883. 10.1016/j.antiviral.2020.104883 . hal-03030827

HAL Id: hal-03030827

<https://hal.science/hal-03030827v1>

Submitted on 22 Aug 2022

HAL is a multi-disciplinary open access archive for the deposit and dissemination of scientific research documents, whether they are published or not. The documents may come from teaching and research institutions in France or abroad, or from public or private research centers.

L'archive ouverte pluridisciplinaire **HAL**, est destinée au dépôt et à la diffusion de documents scientifiques de niveau recherche, publiés ou non, émanant des établissements d'enseignement et de recherche français ou étrangers, des laboratoires publics ou privés.



Distributed under a Creative Commons Attribution - NonCommercial 4.0 International License

Mutations on VEEV nsP1 relate RNA capping efficiency to ribavirin susceptibility

Rabah Nadia^{A,C,*}, Ortega Granda Oney^A, Quérat Gilles^B, Canard Bruno^A, Decroly Etienne^A, Coutard Bruno^{B,*}

^AAix Marseille Université, CNRS, AFMB UMR 7257, Marseille, France

^BUnité des Virus Emergents (UVE: Aix-Marseille Univ-IRD 190-Inserm, 1207-IHU Méditerranée Infection) Marseille, France

^CUniversité de Toulon, 83130 La Garde, France

*Corresponding authors Nadia Rabah and Bruno Coutard

E-mail: bruno.coutard@univ-amu.fr; nadia.rabah@univ-tln.fr

Tel: +33 4 13 73 21 62; +33 4 91 82 55 46

Abstract

Alphaviruses are arthropod-borne viruses of public health concern. To date no efficient vaccine nor antivirals are available for safe human use. During viral replication the nonstructural protein 1 (nsP1) catalyzes capping of genomic and subgenomic RNAs. The capping reaction is unique to the *Alphavirus* genus. The whole three-step process follows a particular order: (i) transfer of a methyl group from S-adenosyl methionine (SAM) onto a GTP forming m^7 GTP; (ii) guanylylation of the enzyme to form a m^7 GMP-nsP1 adduct; (iii) transfer of m^7 GMP onto 5'-diphosphate RNA to yield capped RNA. Specificities of these reactions designate nsP1 as a promising target for antiviral drug development. In the current study we performed a mutational analysis on two nsP1 positions associated with Sindbis virus (SINV) ribavirin resistance in the Venezuelan equine encephalitis virus (VEEV) context through reverse genetics correlated to enzyme assays using purified recombinant VEEV nsP1 proteins. The results demonstrate that the targeted positions are strongly associated to the regulation of the capping reaction by increasing the affinity between GTP and nsP1. Data also show that in VEEV the S21A substitution, naturally occurring in Chikungunya virus (CHIKV), is a hallmark of ribavirin susceptibility. These findings uncover the specific mechanistic contributions of these residues to nsP1-mediated methyl-transfer and guanylylation reactions.

Introduction

Global warming, increased worldwide travel and urbanization, among other causes, promote a significant geographical expansion of many arboviruses, including *Aedes*, *Psorophora* and *Culex* mosquitoes. These arthropods act as vectors for a plethora of causal agents of infectious diseases and thus the emergence and re-emergence of a variety of Alphaviruses is currently observed. Alphaviruses infect diverse hosts including mammals, birds, rodents and salmonids. The genus *Alphavirus* contains 31 species among which 21 were reported to induce pathological symptoms in humans (Weaver et al., 2012). Alphaviruses pathogenic for humans can roughly be divided into two main groups according to the clinical symptoms they trigger. Arthralgic symptoms include fever, cutaneous rash, polyarthralgia and arthritis. They are mainly caused by alphaviruses of the Old World (OW), including Chikungunya virus (CHIKV), O'nyong-nyong virus (ONNV) and Semliki Forest Virus (SFV), with the exception

of Mayaro virus (MAYV) which circulates in the Americas. Conversely, encephalitic symptoms are characteristic of viruses restricted to the New World (NW), such as Eastern, Western and Venezuelan equine encephalitis viruses (EEEV, WEEV and VEEV). They comprise headache, nausea, anorexia and ultimately encephalitis with more than 15% of fatal outcomes. Long-lasting symptoms and the morbidity associated to alphavirus outbreaks make them a serious public health and epizootic threat (Lwande et al., 2015; Zacks and Paessler, 2010). So far, no efficient vaccine nor licenced antivirals are available for safe human use (Abdelnabi et al., 2017). Moreover, the absence of a specific treatment for alphavirus infection limits the therapy, in the case of outbreaks, to the use of medication based mainly on symptoms relieve, such as analgesic, anti-pyretic, anti-inflammatory and immunosuppressing drugs (Sales et al., 2018).

Alphaviruses are enveloped viruses possessing a single positive-stranded genomic RNA. This RNA is first translated by the host cell machinery into polyproteins P123 and P1234 that are subsequently processed by the viral protease yielding proteolytic intermediates and the four non-structural proteins (nsPs) nsP1 to 4. These proteolytic intermediates and the matured nsPs constitute the replication/transcription complexes (RTC) organised in spherules at the plasma membrane. RTC drive the replication of the viral genome but also the transcription and the capping of genomic and subgenomic RNA coding for the structural proteins. NsP1 is the viral RNA capping enzyme, carrying methyl- and guanylyltransferase activities necessary for the viral replication (Ahola and Kaariainen, 1995) (Ahola et al., 1997) (Li et al., 2015). NsP2 possesses NTPase, RNA triphosphatase and RNA helicase activities (Rikkonen et al., 1994) (Law et al., 2019; Vasiljeva et al., 2000). The C-terminal region of nsP2 has a papain-like protease fold and is implicated in the P1234 processing (Hardy and Strauss, 1989; Shirako and Strauss, 1994). NsP3 contains a Macro domain and a C-terminal hypervariable region. The protein nsP4 corresponds to the viral RNA dependent RNA polymerase (RdRp) responsible for RNA synthesis (Chen et al., 2017).

The unique alphaviral replicative process is attractive for the development of potent and specific inhibitors. Several inhibitor screening efforts showed that an antiviral effect can be achieved through targeting a specific nsP. Purine nucleoside analogues or urea-derivatives can inhibit RNA synthesis in SFV, SINV and CHIKV (Albulescu et al., 2015; Delang et al., 2014; Pohjala et al., 2008) (Urakova et al., 2017) , suggesting a direct effect on the nsP4 RdRp. Similarly, formamide-based cysteine protease inhibitors seem promising in targeting CHIKV

and VEEV nsP2 (Das et al., 2016; Hu et al., 2016). The list of active molecules against nsP1 was recently extended with capping inhibitors of different structural classes (Gigante et al., 2014) (Delang et al., 2016) (Feibelman et al., 2018) (Gomez-SanJuan et al., 2018) (Ferreira-Ramos et al., 2019).

In the case of alphaviruses, ribavirin administration to infected patients decreases arthralgia symptoms associated to CHIKV infection (Ravichandran and Manian, 2008). Nevertheless, infection experiments performed in cell lines have evidenced that antiviral effect of ribavirin on alphaviruses is cell-, virus species-, and even virus strain- specific. Hence, CHIKV replication can be inhibited by ribavirin and the antiviral effect is more prominent in hepatoma cells than in lung or kidney cell lines (Franco et al., 2018). In Vero cells, ribavirin has a potent antiviral effect against CHIKV, but also against SINV and Dakar strain of SFV. In contrast, both the Uganda strain of SFV and VEEV species are resistant to ribavirin (Briolant et al., 2004) (De Clercq et al., 1991; Markland et al., 2000). Interestingly, in the same cells, VEEV is sensitive to VX-497, a carbamic acid derivative, targeting IMPDH by uncompetitive inhibition, underlying the high potential of targeting IMPDH in alphavirus infection (Markland et al., 2000).

Sheidel and Stollar isolated SINV mutants resistant to three inhibitors of IMPDH, namely MPA, ribavirin and 2-amino-1,3,4-thiadiazole. The reported mutants had a 3 000 fold increased viral load when challenged with the drug compared to the WT. Genomes of resistant mutants carried three non-synonymous mutations in the nsP1 coding sequence, yielding the amino acid substitutions Q21K, S23N and V302M (Scheidel et al., 1987) (Rosenblum et al., 1994). Positions 21 and 23 are in the vicinity of another resistant mutation selected against the capping inhibitors [1,2,3]triazolo[4,5-d]pyrimidin-7(6H)-ones bearing antiviral activity (Delang et al., 2016). Together, these observations suggest that the inhibition of IMPDH affects indirectly viral capping. The nsP1 promotes specific RNA capping in the following order: (i) a methyltransferase reaction (MTase), where GTP + SAM form m^7 GTP and the S-adenosylhomocysteine (SAH) by-product (ii) A first guanylyltransferase reaction (GTase1), where the enzyme forms a covalent complex m^7 GMP-nsP1. (iii) a second guanylyltransferase reaction (GTase2), where the m^7 GMP is transferred onto a 5'-diphosphate RNA (ppRNA), to form the cap structure m^7 GpppRNA (Li et al., 2015).

In this study, we focus on VEEV nsP1 Q19 and S21 residues, which correspond to the SINV ribavirin resistant mutants mentioned above. We have generated different combinations of K,

N and A substitutions both in the VEEV reverse genetics system and nsP1 recombinant enzyme in order to elucidate the role of these amino acids in the viral capping and the viral susceptibility/resistance towards the compounds regulating the intracellular GTP pool. Our data demonstrate that: (i) By modulating SAM and GTP binding, Q19 is a key residue for the MTase reaction; (ii) S21 is essential for ^{m7}GMP-nsP1 complex formation during the GTase1 reaction; (iii) The double mutant Q19K-S21N, leads to a 3-fold increase in GTase2 activity. (iv) S21A substitution, corresponding to the naturally occurring CHIKV polymorphism, is a hallmark of ribavirin susceptibility.

Materials and Methods

Cloning, mutagenesis and expression of VEEV nsP1 proteins

The DNA sequence corresponding to the VEEV nsP1 protein (strain P676, amino acid 1 to 535) was synthesized by GenScript and cloned into the pET28b (Novagen) vector in fusion with a C-terminal hexa-histidine tag after codon optimization for bacterial expression. Site-directed mutagenesis was performed by PCR amplification of the WT sequence with primers carrying the desired mutations and using PFU Turbo (Ambion) as described by the manufacturer's protocol. All constructs were confirmed by DNA Sanger sequencing. T7 Express *E. coli* (NEB) were transformed by the VEEV nsP1 expressing plasmids and grown at 37°C in Terrific Broth medium until an OD_{600nm} reached 0.6. Induction of protein expression was carried with 0.5 mM isopropyl-β-d-thiogalactopyranoside (IPTG, Sigma) for 3 hours at 17°C. Cells were harvested by centrifugation at 5,000 x g for 15 min. The pellets were stored at -80°C until purification.

Protein purification

Bacteria pellets were thawed on ice, then lysed in 20 mM Tris-HCl pH7.5, 300 mM NaCl, 5% glycerol, 5 mM mercaptoethanol supplemented with 20 μg/ml DNase I, 0.25 mg/ml lysozyme and Complete EDTA-free Protease Inhibitor Cocktail (Sigma). After complete dissolution of the pellet, samples were sonicated and clarified by centrifugation (30 000 x g for 30 min at 4°C). Following the addition of imidazole to a final concentration of 40 mM, soluble fractions were incubated with Ni-Sepharose resin (GE Healthcare; 0.5 ml/l culture) for 1 h at 4°C, with gentle shaking. Beads were washed 2 times with 5 column volumes (CV) of lysis buffer then 5 CV of wash buffer (20 mM Tris- HCl, pH 7.5, 1 M NaCl, 5% glycerol, 40 mM imidazole). Proteins were eluted in 20 mM Tris-HCl pH 7.5, 300 mM NaCl, 5% glycerol, 250 mM imidazole. Finally, proteins were concentrated using Amicon Ultra (EMD Millipore) ultrafiltration units and dialysed against storage buffer (20 mM Tris-HCl pH 7.5, 100 mM NaCl, 50% glycerol) for storage at -20°C.

Methyltransferase assay

The transfer of the methyl group from S-adenosyl-[methyl-3H] methionine (SAM [H³]) (PerkinElmer) to GTP or guanylylimidodiphosphate (GIDP) was performed as described previously (Li et al., 2015). Briefly, 5μM of VEEV nsP1 WT and mutant were incubated in 50 mM Tris pH 7.0, 2 mM DTT, 10 mM KCl, 2 mM MgCl₂, 2 mM GTP or GIDP, 0.55 μCi

(SAM [H^3]) (0.33 μ M), at 30°C. The reaction was stopped by loading the samples on DEAE-cellulose filters (PerkinElmer). The filters were washed twice with 10 mM ammonium formate, once with H₂O, and finally with 95% ethanol. The radioactivity was measured by scintillation counting with SCINT BETAPLATE solution in a MicroBeta 2 counter (PerkinElmer). The kinetics parameters were determined by varying the concentrations of either SAM, GTP or GIDP. Data were analysed using Sigmaplot software.

nsP1 guanylyltransferase assay (GTase1)

The formation of m^7 GMP-nsP1 complex was monitored by incubating 5 μ M of each VEEV-nsP1 protein with [α -P³²] GTP (3000 Ci/mmol), 100 μ M SAM, 10 mM NaCl, 2 mM MgCl₂ and 2 mM DTT in 20 mM HEPES buffer pH 7, at 30 °C for 1 h. The complex was then resolved by electrophoresis on a 12% SDS-PAGE. The radiolabeled material was visualized using Amersham Typhoon phosphor-imager.

***In vitro* transcription**

DNA oligonucleotide corresponding to the first 30 nucleotides of VEEV genomic RNA preceded by the phi 2.5 class II promoter was used as a template in an *in vitro* RNA reaction synthesis. Transcription buffer contained 40 mM Tris-HCl (pH 7.0), 40 mM MgCl₂ and 2 mM Spermidine, 0.01% Triton, 4% PEG 8000. The reaction was conducted at 37°C for 4h in the presence of 8 mM of NTPs (GE Healthcare), T7 RNA polymerase (0.1 μ M) and RNase inhibitor (Ambion). The RNA solution was centrifuged 15 min at 3000 x g, treated with 15 min at 37°C with DNase (Ambion), then subjected to a phenol/chloroform extraction. RNA was subsequently precipitated with ethanol supplemented with 2.5 M of Ammonium acetate O/N at 4°C. The purified RNA is hereafter named VEEV RNA.

RNA guanylyltransferase assay (GTase2: formation of m^7 GpppRNA)

In order to remove the γ -phosphate of T7 expressed RNA, 5 μ M of VEEV RNA was preincubated with 1 μ M of Dengue NS3, produced and purified as described previously (Milhas et al., 2016) in 50 mM HEPES (pH 7.5) and 2 mM DTT for 30 minutes. The reaction was stopped by heat inactivation at 65 °C for 5 min. The generated diphosphate 5' termini VEEV RNA was then incubated with 2 μ M of nsP1 VEEV proteins in a reaction mixture containing 10 μ Ci of [α -P³²] GTP (3000 Ci/mmol), 50 mM HEPES (pH 7.5), 10 mM KCl, 2 mM MgCl₂, 2 mM DTT and 100 μ M SAM for 2 h at 30°C. After one freezing/ thawing cycle the capped RNAs were digested with 1 U of nuclease P1 (Sigma) in 30 mM sodium acetate

(pH 5.3), 5 mM ZnCl₂ and 50 mM NaCl (2 h, 37°C). At the end of the reaction, proteins were hydrolysed with 1 U of proteinase K (NEB). Digestion products were separated by polyethylenimine cellulose thin-layer chromatography (Macherey-Nagel) and resolved using 0.45 M (NH₄)₂SO₄ as mobile phase. The radiolabeled material was visualized as described above.

Generation of a recombinant VEE virus

Wild type and mutants VEEV were generated by co-transfection in Vero E6 cells of overlapping synthetic (GenScript) molecular clones covering the whole genome using the Infectious Subgenomic Infectious Amplicons (ISA) method as previously described (Aubry et al., 2015). Briefly, Three VEEV fragments were generated. The first 5' end fragment covers the CMV early promoter linked to the first 80 nucleotides of the VEEV genome (strain P676). The second fragment encompasses either WT or mutated nsP1 from nucleotide position 1 to position 1772 of the VEEV genome. The third fragment encompasses Nsp2 to Nsp4 from nucleotide position 1683 to 7583 and the 3' end fragment encompasses the structural proteins and the 3' UTR (7503 to genome end) linked to a poly A tail, a ribozyme site and the SV40 poly A signal. All fragments were linearized by amplification from the GenScript-delivered plasmid using Taq polymerase and directly purified from the amplification reaction. The day before transfection Vero E6 cells were seeded in 96 wells plates at 50000 cells per well. Transfection was carried using Lipofectamine 3000 reagent (Life Technologies) and 100 ng of total DNA per well. Supernatants were collected on day 6 post transfection. Viral genomes were quantified by quantitative RT-PCR of viral RNA extracted from the supernatant in presence of a DNase treatment. Subsequently, viral stocks were grown on Vero cells.

Antiviral assay

Antiviral assays were performed using recombinant VEEV WT, S21A (see above) and Chikungunya virus strain Opy1 (La Réunion Island LR2006_OPY1; EVAg 001v-EVA83). The amount of each virus and the duration of the assay had initially been calibrated so that the replication is still in the log phase of growth at the time of readout and the cycle threshold (CT) standard deviations of qRT-PCR quantification (quadruplicate) is below 0.5. Approximate multiplicity of infection (MOI) range from 10⁻⁴ to 10⁻³ depending on the strain.

One day prior to infection 5×10^4 Vero E6 cells were seeded in 100 μ l of medium (supplemented with 2.5 % FCS) in each well of a 96-well titer plate. The next day, 8 two-fold serial dilutions of the compounds (beginning at 400 μ M final concentration, down to 0.16 μ M), in duplicates or triplicates, were added to the cells (25 μ l/well, in 2.5 % FCS containing medium). Four Virus Control (VC) wells (per virus) were supplemented with 25 μ l medium. Fifteen minutes later, 25 μ l of a virus mix containing the appropriate amount of viral stock diluted in medium (2.5 % FCS) were added to the 96-well plates.

Cells were cultivated for 36 to 48 hours after which 100 μ l of the supernatant were collected for viral RNA purification. The supernatants were transferred to 96 well S-Bloc from QIAgen preloaded with VXL mix and extract by the Cadon Pathogen 96 QIAcube HT kit run on QIAcube HT automat according to Qiagen protocol. Purified RNAs were eluted in 80 μ l of water. Viral RNAs were then quantified by real time one step RT-PCR to determine viral RNA yield using 3.5 μ l of RNA and 6.5 μ l of RT-PCR mix using standard cycling parameters. The four control wells were replaced by four 2 log dilutions of an appropriate T7-generated RNA standards of known quantities for each viral genome (100 copies to 100 million copies).

Mean inhibition of virus yield is equal to $100 \times (\text{mean quantities of viral RNA in VC quadruplicates} - \text{mean quantities of viral RNA in drug treated triplicates}) / \text{mean quantities of viral RNA in VC}$. The inhibition values (expressed as percent inhibition, in linear scale) obtained for each drug concentration (expressed in μ M, in log scale) are plotted using Kaleidagraph plotting software (Synergy Software) and the best sigmoidal curve, fitting the mean values, is determined by a macro in the software: (Inhibition, Y is given by $Y = 100 / (1 + (m_0/m_1)^{m_2})$). This macro allows to determine the best curve fit and the m_1 and m_2 parameters, where m_1 corresponds to EC_{50} .

Results

The aim of this study was to examine the effect of nsP1 mutations both in infected cells and at the enzyme level in order to get mechanistic insights into the alphavirus RNA-capping process. In SINV, three mutations in nsP1 were shown to be associated to ribavirin resistance (Figure 1): (i) a glutamine (Q) to a lysine (K) in position 21; (ii) a serine (S) to an asparagine (N) at position 23 and (iii) a valine (V) to a methionine (M) in position 302. These substitutions induced a cross-resistance to ribavirin and 2-amino-1,3,4-thiadiazole, both inhibitors of the cellular enzyme IMPDH. These data might suggest that cellular GTP pool balance is a concern in resistance development through a potential nsP1 capping activity modulation. In order to refine the role of these amino acids and their substitutions, we first assessed the molecular context associated to ribavirin resistance by an alignment analysis restricted to the three loci involved in ribavirin-resistance in the SINV model (Figure 1). Position 21 is occupied by a conserved glutamine (Q) along the human-tropic alphaviruses. In contrast, the amino acid at position 23 is varying following the geographical distribution of human-tropic alphaviruses, with an alanine (A) for OW viruses and with a polar residue serine (S), threonine (T) or cysteine (C)) for NW viruses. In position 302, the amino acid can greatly vary with no obvious relation with the geographical distribution. We therefore decided to focus the study on positions 21 and 23 corresponding to residues 19 and 21 on the VEEV nsP1 sequence, respectively. Hence we mutated Q19 and S21 to various combinations of K, N and A residues, both in the VEEV reverse genetics system, and in the recombinant VEEV nsP1 protein for biochemical characterization, VEEV nsP1 being the biochemical model validated for all the capping steps (Li et al., 2015).

Effect of the mutations on methyltransferase activity (MTase)

To understand the effect of substitutions at positions 19 and 21, we first examined the effect of these mutations on nsP1 methyltransferase activity using time course experiments. For this purpose, the different mutant proteins were incubated with GIDP, a non-hydrolysable analogue of GTP, in the presence of [³H] SAM, and the enzymatic activity was determined using a filter binding assay. Figure 2A shows a time course experiment indicating that under these conditions all mutants are in the linear phase of the reaction before 180 min. Figure 2B represents a 2 hours end-point assay summarizing the resulting effects of the mutations and

allowing the comparison of measured MTase activities relative to that of the WT enzyme. It appears clearly that most of the mutants display a decreased activity compared to the WT except Q19K and S21A. Mutants can be divided in two groups. A first group with decreased enzymatic activity compared to the WT including Q19N and Q19A, these latter keep about 50% of the nsP1 MT activity (Figure 2A and B and Table I). The other mutants from this group (S21N, Q19K /S21N and Q19N /S21N) show a marked decreased (70-80%) of MT activity. All of them contain the S21N substitution. This observation suggests that activity loss is the hallmark of S21N substitution. Mutants of the second group present an enhanced MTase activity, with Q19K and S21A single mutations, yielding up to 1.57 time increase of the activity. However, it is noteworthy that the increase of the activity due to Q19K cannot compensate the negative effect of S21N. Altogether these results suggest that the loci on the nsP1 sequence studied here contains residues impacting the methyltransferase activity, relating MPA- and Ribavirin-resistance to this enzyme.

To date no crystal structure of alphavirus nsP1 is available. NsP1 has a predicted Rossmann fold with canonical motifs in its N-terminal domain, and is putatively folded with α -helices and β -sheets separated by loops probably involved in nucleotide co-factor binding (Ahola et al., 1997) (Ahola and Karlin, 2015). In order to define if the targeted mutations regulate either GTP and/or SAM binding, we determined the apparent K_m values for SAM and GIDP. Briefly, we quantified the amount of [3H] methyl transferred on GIDP at increasing concentration of SAM or GIDP and the K_m was deduced from Lineweaver-Burk plots (Figure 2 C and D). The kinetic experiments indicate that WT nsP1 binds SAM with an apparent K_m of 0.5 μ M (Table II) which is in the same range as the K_m of other previously characterized recombinant MTases (0.1 to 8 μ M) (Schulz and Rentmeister, 2012; Tomar et al., 2011) (Horiuchi et al., 2013). The K_m value of mutant nsP1 varies between 0.14 and 1.5 μ M. These values are barely impacted by single mutations except for Q19K showing a ~3-fold increase in SAM binding. Increased SAM binding properties of this mutant correlates with increased MTase activity (Figure 2). Conversely, the double mutant (Q19K/S21N and Q19N/S21N) show a ~3-fold increased K_m , which might explain the reduced MTase activity of these mutants. The K_m value of WT nsP1 VEEV for GIDP was also determined (0.27 mM, Figure 2E). The K_m values of mutant proteins vary from 0.1 to 0.6 mM, except for S21A nsP1 which shows a K_m at 10 μ M, reflecting a 27-fold increased apparent affinity for the GTP analogue compared to that of WT. This dramatic change might explain the enhancement of the corresponding MTase activity observed in Figure 2D and C. Altogether these results

indicate that position 19 and 21 of VEEV nsP1 impact both SAM and GIDP binding. In addition, we observe that mutations increasing the SAM or GIDP binding properties increase the MTase activity of nsP1 whereas those decreasing SAM or GIDP recruitment decrease the MTase activity.

Effect of mutations on nsP1-guanylylation (GTase1)

We next wanted to determine whether the mutants could differentially affect the formation of the ^{m7}GMP-nsP1 adduct. To test this hypothesis we incubated each mutant in the presence of SAM and [α -³²P] GTP. During the incubation, the [α -³²P] GTP is first methylated on its N7 position (MTase reaction) and the guanylylation of nsP1 occurs subsequently (GTase1 reaction). The generated radiolabeled ^{m7}GMP-nsP1 complex was next separated using SDS-PAGE and the amount of [α -³²P] GTP bound to nsP1 was quantified. Figure 3 shows that Q19K and S21A single substitutions result in a 2-fold increase of complex formation compared to that of WT nsP1. This is reminiscent of the increased MTase activity observed above (Figure 2). The S21N mutation either alone or associated to Q19K or Q19N significantly decreases nsP1-guanylylation as observed for the MTase reaction. In contrast, the Q19A mutant which is characterized by moderate MTase activity shows an increase in nsP1 guanylylation, since its activity is similar to WT. Indeed, since MTase and nsP1-guanylylation reactions are sequential, this result suggests that the MTase reaction is not rate-limiting for this mutant. Hence, the assessment of the GTase1 reaction *per se* for each individual mutant can be evaluated by calculating the ratio global ^{m7}GMP-nsP1 complex formation /MTase (Table I). By doing so one can notice that mutating Q19 to K but not N increases nsP1-guanylylation (25%). In addition we calculated an increase of about 50% for the S21A mutant and almost 100% (2-fold), for Q19A and S21N. Interestingly, it seems that there is no synergistic effect between the two residues for the GTase1 reaction, since the double mutants behave almost identically to the corresponding single Q19 mutant.

Effect of mutations on RNA-guanylyltransferase activity (GTase2)

Subsequently, we explored the effect of amino acid substitutions on the nsp1-mediated RNA-guanylylation reaction leading to the formation of the ^{m7}GpppRNA cap structure (GTase2 reaction). To assess this reaction, the first 30 nucleotides corresponding to the 5' sequence of VEEV genomic RNA were *in vitro* transcribed and the 5'-triphosphate end of RNA was

dephosphorylated to generate a 5'-diphosphate end. We then incubated this RNA with nsP1 mutants, SAM and [α - 32 P] GTP. The reaction products - capped RNAs - were next digested by P1 endonuclease treatment. The released cap structures were separated using thin layer chromatography (TLC), and revealed by autoradiography (Figure 4). Typically, TLC profiles reveal the presence of all nucleotide moieties present during the different steps of the reaction, namely GTP, GDP, GMP, m^7 GTP and the cap structure m^7 GpppA. For the negative control (without nsP1) the main product observed is GTP, although faint spots corresponding to GDP and GMP are present, generated by GTP hydrolysis. When nsP1 enzymes are present, GTP, GDP and GMP all the above mentioned chemical species are still present. In particular GDP is a well-known by-product of the cap synthesis mediated by the the Bamboo mosaic virus capping enzyme (Hu et al., 2011; Huang et al., 2004; Lin et al., 2012). The m^7 GTP is the product of the MTase reaction and migrates very close to GMP. Lastly, the m^7 GpppA cap structure corresponds to the final product of the global capping reaction. The intensity of the m^7 GpppA product differs from one mutant to another and reflects the effect of the mutations on the global capping reaction. Figure 4 points out that the substitution to N of one or both Q19 and S21 residues negatively affects the overall capping reaction. Q19A substitution induces a 20% gain over the WT nsP1 capping activity. Strikingly, Q19K and S21A induce a 2.5-fold increase in capping compared to the WT nsP1. Still, the activity described above corresponds to the global capping activity including MTase, GTase1 and GTase2 activities. When looking at the ratio of GTase2 over GTase1 (Table I), one can estimate the rate of the GTase2 reaction *per se* for each mutant. Hence, the substitution of one residue leads to a 1.5 to 2-fold rise in GTase2 activity. Q19 and S21 residues appear to act in synergy, since the double mutants are 2.5 to 3-fold more active than the WT. It should be emphasised that the guanylyltransferase activity of nsP1 comprising the formation the m^7 GMP-nsP1 complex and the transfer to RNA is increased for all the mutants.

Effect of ribavirin on WT and S21A VEEV replication

To investigate the role of Q19 and S21 nsP1 VEEV residues on ribavirin susceptibility, we next introduced the mutations of interest into the VEEV molecular clone using the ISA method in Vero E6 cells (Aubry et al., 2015). Unfortunately, in this system only S21A substitution led to the generation of viable viral particles. The other substitutions yielded no or low-efficiency replicating viruses, insufficient to initiate an antiviral assays in the presence

of ribavirin (data not shown). Therefore, the analysis focused on VEEV WT and S21A, using CHIKV as reference. To test the effect of ribavirin on these viruses, the amount of viral RNA in infected cultures containing increased amounts of ribavirin was compared. The dose response curves are presented in Figure 5 and EC_{50} compiled in Table III. As expected, VEEV WT is not sensitive to ribavirin below 250 μ M, whereas EC_{50} of ribavirin on CHIKV could be determined and is about $26 \pm 8 \mu$ M (Table III). Interestingly, VEEV S21A became ribavirin sensitive in the assay, with EC_{50} of $60 \pm 13 \mu$ M. In the genomic sequence of CHIKV the naturally occurring residue at that position is an A (Figure 1). This observation suggests that this position might be one of the hallmarks towards ribavirin sensitivity in alphaviruses. To confirm that the antiviral effect of ribavirin is associated to the inhibition of the cellular IMPDH, the experience was repeated using a culture medium supplemented with GMP. Exogenous supply of GMP allows to bypass the IMPDH pathway and partly restores GTP synthesis. In the presence of exogenous GMP, the antiviral effect of ribavirin is partly abrogated for both CHIKV and VEEV S21A, suggesting that ribavirin effect on both viruses is mediated through IMPDH inhibition.

Discussion

The results presented here support the initial hypothesis according to which the development of resistance following GTP depletion is associated to a modulation of the capping efficiency. Hence, mutation of Q19 to K led to a three fold increase in SAM and GTP affinity, thereby enhancing the first step of the capping pathway, *i.e.*, the MTase reaction. The importance of this specific lysine in the GTP methylation is supported by the fact that substitution of Q19 to N has nearly no effect on SAM and GTP kinetic parameters. It is noteworthy that K in position 19 selected in SINV ribavirin resistant virus is also naturally observed in the fish alphaviruses SPDV and SDV, reflecting possible discrepancies of GTP concentration in the intracellular environment between mammal- and fish-infecting alphaviruses. The only example in the literature where a nearby residue was mutated is the substitution of L18 to E (L19E) in SFV nsP1, which leads to the complete and partial loss of SAM and GTP binding in UV-crosslinking experiments, respectively (Ahola et al., 1997). Concerning position 21, the results suggest that this residue regulates the guanylylation reaction. The S21N substitution has a weak MTase activity but a strong nsP1 guanylylation activity (GTase1). When acting in synergy with the K in position 19, the RNA guanylylation (GTase2) is

increased up to 207% vs 117% and 125% for the single mutants. This phenomenon endorses the resistance mutations observed in SINV, in which upon GTP depletion the adaptive response could be the generation of an enzyme with higher GTP affinity and a stronger cap transfer on RNA. This hypothesis would have however to be validated on SINV nsP1 model.

Our results point out to a close interconnection between GTP and SAM binding, as evidenced by the kinetic parameters determined for each substrate. This observation is also in agreement with previous studies highlighting that SAH produced during methylation is regulating the downstream steps of the capping (Li et al., 2015). From a structural point of view, these data support the fact that the two binding sites could be close to each other and involve leaning residues in the extreme N-terminus of the MT domain, as illustrated in the structure of Flavivirus virus (ZIKV) NS5 protein (Coutard et al., 2017; Zhao et al., 2017).

In parallel, we show that some polymorphism exists at position 21 in the alphavirus family (Figure 1). We established that S21A shows an increased sensitivity of VEEV to ribavirin. As the addition of GMP decreases the antiviral effect of ribavirin, we assume that S21 might represent a key residue in ribavirin susceptibility. Together with the increase of the susceptibility towards ribavirin, S21A substitution on recombinant VEEV nsP1 shows a strong MTase activity and a 2-fold increased guanylyltransferase activity. This substitution, which is OW alphavirus specific (Figure 1) points out that there are differences in the molecular mechanism governing capping reaction between alphavirus members. However, it remains possible that drug resistance/sensitivity could be modulated by compensatory mutations in other nsPs which remain to be determined.

Hence, it is important to bear in mind that drug resistance can be concomitant to mutations in other nsPs. Compensatory mutations are mainly due to the dynamic of interactions between the various nsPs alone or in the context of different polyprotein state in the course of processing, as exemplified by the switch between negative and positive sense RNA synthesis (Lemm et al., 1994). Recent study on Favipiravir, a potent antiviral pyrazine derivative against alphaviruses, led to the isolation of CHIKV nsP4 K291R resistant mutation. This mutant could not survive in the absence of the drug unless compensatory mutations in nsP2 and nsP3 were present (Delang et al., 2014). In SINV, synergic effect of compensatory mutations between nsP1 and nsP4 was observed in methionine depletion resistant mutants (Stollar et al., 2013). Moreover, subjecting VEEV infected cells to cytidine analog, β -D-N4-hydroxycytidine, showed that it has a strong antiviral potential. However, virus developed

resistance mutations in nsP4, explained by its role in nucleotide incorporation, but also to a lesser extent into all other nsPs (Urakova et al., 2017).

Interestingly, ribavirin resistance was generally associated to mutations in viral RdRp domains. These mutations could be explained by the triphosphate form of ribavirin acting as an obligate or non-obligate chain terminator for the polymerase, or by the monophosphate form of ribavirin inhibiting IMPDH and inducing the depletion of GTP together with hypermutation by lack of available nucleotide (De Clercq and Li, 2016). However, other mode of action of ribavirin has emerged in certain virus family, with some of them targeting the cap formation. For example, ribavirin 5'-triphosphate was crystallized into the GTP-binding site of the DENV MTase NS5 (Benarroch et al., 2004). Likewise, a direct interaction of ribavirin with vaccinia virus (VV) capping D1 subunit was described. The monophosphate of ribavirin is able to form a RMP-D1 complex leading to the formation of RpppRNA (Bougie and Bisailon, 2004). The characterization of the L protein of different rhabdoviruses showed that ribavirin diphosphate (RDP) could also bind the GDP polyribonucleotidyltransferase domain and interfere with cap formation only if the concentration of cellular GDP is low (Ogino and Ogino, 2017). Moreover, we and others have shown that 5'-triphosphate ribavirin is not acting directly on nsP1, as demonstrated by mM range IC_{50} values for VEEV and CHIKV nsP1 MTase (Kaur et al., 2018; Li et al., 2015). A similar IC_{50} value was obtained for VEEV nsP1 when tested in GTase 2 assay in the presence of RTP (data not shown).

RNA capping is a crucial process for controlling RNA stability, translation and recognition of "self" by host cells. Diphosphate, triphosphate, mis-capped or mis-folded RNA trigger the activation of RIG-I, MDA 5 and toll like receptors (TLR7/8 and TLR3) leading to Interferon secretion and thereby to the restriction of mis-capped viral genomes (Freund et al., 2019; Hyde et al., 2014). This is emphasised in different studies. In reoviruses for example increased infectivity can be associated with improved vRNA capping (Eaton et al., 2017). Likewise, Flaviviruses can boost their guanylation activity under oxidative stress conditions to enhance viral replication (Gullberg et al., 2015). In alphaviruses, the situation appears puzzling. In general, drug resistance mutations observed in alphavirus nsPs (including those studied here; see above) decrease viral infectivity and negatively impact viral replication. This translates into small viral plaques and reduced viral titers in resistant mutants (Scheidel and Stollar, 1991; Urakova et al., 2017). Hence, point mutations leading to an increased nsP1 activity suggest that over-capping has a deleterious effect on the efficiency of viral infection

(LaPointe et al., 2018; Stollar et al., 2013). During alphavirus replication, viral RNA population is heterogeneous. In addition to capped viral RNA, the infection leads to the accumulation of mono, di, tri and even non phosphate viral RNA. Interestingly, capped and uncapped RNA can be encapsidated with or without host's translation factors (Sokoloski et al., 2015). Clearly, the balance between capped and uncapped viral RNA is an important issue, whose biological significance is still to be defined. Over-capping might lead to a competition over translational host factors with a negative impact on infectivity. Yet in the case of drug-induced GTP pool depletion, the maintenance of an appropriate ratio of capped/uncapped RNA could be achieved by capping increase.

In conclusion, our results suggest that positions 19 and 21 are key players in the capping mechanism. In the presence of IMPDH inhibitors, RNA capping can be enhanced by mutations of these residues in order to overcome GTP depletions. The nature of the amino acid at position 21 might represent an important sensitivity/resistance marker to be taken into account for the rational design of nsP1 inhibitors.

Acknowledgments

Oney Ortega is a recipient of Infection Méditerranée Infection Fondation studentship.

Captions

Figure 1 : Multiple sequence alignment of alphavirus nsP1 proteins in the vicinity of ribavirin resistance mutations. Sequence alignment was performed using T-Coffee and combined to PHD secondary-structure prediction using the ESPript software. Sequence of VEEV is numbered. Sites of ribavirin resistance mutations are in red boxes. Catalytic histidine is highlighted in the blue box. Black squiggles and arrows represent α helices and β strands respectively. Dotted lines indicate region with low reliability of secondary structure elements for α helices and β strands. VEEV, Venezuelan equine encephalitis virus (NC_001449.1); SINV, Sindbis virus (NC_001547.1) ; AUV, Aura virus (NP_819010.1); ONNV, O'nyong-nyong virus (NC_001512.1); CHIKV, Chikungunya virus (MH229986.1); SFV, Semliki Forest virus (NC_003215.1); MAYV, Mayaro virus (AZM66145.1); BFV, Barmah Forest virus (NC_001786.1); EEEV, Eastern equine encephalitis virus (KX029319.1); WEEV, Western equine encephalomyelitis virus (NC_003908.1).

Figure 2: Altered methyl-transfer in mutated nsP1. The activity was monitored by incubating VEEV-nsP1 WT and mutant proteins at 30°C for varied amounts of time in the presence of 50 mM Tris (pH 7.0), 2 mM DTT, 10 mM KCl, 2 mM MgCl₂, 2 mM GTP or GIDP, 0.55 μ Ci (SAM [H₃]). The reaction product was loaded on DEAE-cellulose filters and the radioactivity quantified by scintigraphy. The mutation effect was investigated either in time course (A) or 2 hours end-point experiments (B). (C) Typical Michaelis-Menten and Lineweaver –Burk plot for WT nsP1VEEV. Kinetic parameters were determined using Sigmaplot program and compiled in Table II.

Figure 3: Effect of mutations on the formation of m⁷GMP-nsP1 complex. A: nsP1 guanylylation was monitored by SDS-PAGE following m⁷-GMP-nsP1 complex formation using [α -P³²] GTP, 100 μ M cold SAM and 5 μ M of each nsP1 enzyme. B: Coomassie blue stained gel of the nsP1-guanylylation reaction for protein load normalisation. C: Relative activity of VEEV nsP1 WT and mutant enzymes.

Figure 4: Impact of ribavirin resistant mutation on RNA Guanylyltransferase activity. A. VEEV-RNA guanylylation reaction was carried out in the presence of diphosphate 5' termini VEEV RNA 30 oligomer nucleotides, 2 μ M of nsP1, 100 μ M of SAM and 0.33 μ M of [α - P³²] GTP. m⁷GpppA caps were digested from RNA with nuclease P1 and resolved on

polyethylenimine cellulose thin-layer chromatography. B. The relative activity was calculated by considering that of WT as 100%. Values correspond to means \pm standard deviation. See Material and method for detailed procedure.

Figure 5: Dose response curves of ribavirin on the replication of CHIKV, VEEV WT and VEEV S21A, in presence or absence of GMP.

Table I: Effect of mutations on the capping reactions.

Table II: Effect of mutations on kinetic parameters for MTase reaction

Table III: Antiviral activity of ribavirin on VEEV WT and S21A.

Table I: Effect of mutations on the capping reactions.

VEEV nsP1	Methyltransferase MTase (%)^a	m⁷GMP-nsP1 complex GTase 1 (%)^b	RNA guanylylation GTase 2 (%)^c	Guanylyltansferase activity GTase 1+GTase 2 (%)^d
WT (Q19/S21)	100	100	100	100
Q19K	157±6	124	117	145
Q19N	55±6	85	197	167
Q19A	58±3	195	107	209
S21A	137±2	147	136	200
S21N	33±4	191	125	239
Q19K /S21N	31±7	126	207	261
Q19N /S21N	22±2	91	350	318

Note: (a) m⁷GDP formation refers to the methyltransferase reaction in the presence of 5 μM WT or mutant nsP1, 0.33 μM of SAM [H³] and 2mM of GDP. Values correspond to means of three different experiment ± standard deviation. (b) GT1 activity corresponding to the ratio of m⁷GMP-nsP1 complex formation (Figure 3) vs MT activity, assuming that all the formed m⁷GTP is used in the reaction. (c) GT2 activity corresponding to the ratio of m⁷GpppA formation (Figure 4) vs GT1 activity. (d) Total guanylylation reaction corresponding to the ratio of RNA-guanylylation vs MT activity.

Table II: Effect of mutations on kinetic parameters for MTase reaction

VEEV nsP1	K_m (SAM) (μM)	K_m (GDP) (mM)
WT	0.55±0.16	0.27±0.08
Q19K	0.14±0.03	0.1±0.02
Q19N	0.5	0.23±0.1
Q19A	0.75±0.3	0.65±0.2
S21A	0.58±0.1	0.01±0.003
S21N	0.71±0.05	0.2±0.002
Q19K /S21N	1.54±0.4	0.11±0.07
Q19N /S21N	1.3±0.3	0.08±0.02

Note: Kinetic parameters were calculated from Lineweaver –Burk plots using Sigmaplot program.

Table III: Antiviral activity of ribavirin on VEEV WT and S21A.

EC ₅₀ (μM)	VEEV WT	VEEV S21A	CHIKV OPY1
Ribavirin	> 270	60±13	26±8
Ribavirin+ 100 μM GMP	> 400	> 400	90±18

Note: EC₅₀ was determined as the mean of the results from three independent experiments (ribavirin alone) and duplicates (Ribavirin+ 100 μM GMP).

Bibliography

- Abdelnabi, R., Neyts, J., Delang, L., 2017. Chikungunya virus infections: time to act, time to treat. *Curr Opin Virol* 24, 25-30.
- Ahola, T., Kaariainen, L., 1995. Reaction in alphavirus mRNA capping: formation of a covalent complex of nonstructural protein nsP1 with 7-methyl-GMP. *Proc Natl Acad Sci U S A* 92, 507-511.
- Ahola, T., Karlin, D.G., 2015. Sequence analysis reveals a conserved extension in the capping enzyme of the alphavirus supergroup, and a homologous domain in nodaviruses. *Biol Direct* 10, 16.
- Ahola, T., Laakkonen, P., Vihinen, H., Kaariainen, L., 1997. Critical residues of Semliki Forest virus RNA capping enzyme involved in methyltransferase and guanylyltransferase-like activities. *J Virol* 71, 392-397.
- Albulescu, I.C., van Hoolwerff, M., Wolters, L.A., Bottaro, E., Nastruzzi, C., Yang, S.C., Tsay, S.C., Hwu, J.R., Snijder, E.J., van Hemert, M.J., 2015. Suramin inhibits chikungunya virus replication through multiple mechanisms. *Antiviral Res* 121, 39-46.
- Aubry, F., Nougairède, A., de Fabritus, L., Piorkowski, G., Gould, E.A., de Lamballerie, X., 2015. "ISALation" of Single-Stranded Positive-Sense RNA Viruses from Non-Infectious Clinical/Animal Samples. *PLoS One* 10, e0138703.
- Benarroch, D., Egloff, M.P., Mulard, L., Guerreiro, C., Romette, J.L., Canard, B., 2004. A structural basis for the inhibition of the NS5 dengue virus mRNA 2'-O-methyltransferase domain by ribavirin 5'-triphosphate. *J Biol Chem* 279, 35638-35643.
- Bougie, I., Bisailon, M., 2004. The broad spectrum antiviral nucleoside ribavirin as a substrate for a viral RNA capping enzyme. *J Biol Chem* 279, 22124-22130.
- Briolant, S., Garin, D., Scaramozzino, N., Jouan, A., Crance, J.M., 2004. In vitro inhibition of Chikungunya and Semliki Forest viruses replication by antiviral compounds: synergistic effect of interferon-alpha and ribavirin combination. *Antiviral Res* 61, 111-117.
- Chen, M.W., Tan, Y.B., Zheng, J., Zhao, Y., Lim, B.T., Cornvik, T., Lescar, J., Ng, L.F.P., Luo, D., 2017. Chikungunya virus nsP4 RNA-dependent RNA polymerase core domain displays detergent-sensitive primer extension and terminal adenylyltransferase activities. *Antiviral Res* 143, 38-47.
- Coutard, B., Barral, K., Lichiere, J., Selisko, B., Martin, B., Aouadi, W., Lombardia, M.O., Debart, F., Vasseur, J.J., Guillemot, J.C., Canard, B., Decroly, E., 2017. Zika Virus Methyltransferase: Structure and Functions for Drug Design Perspectives. *J Virol* 91, e02202.
- Das, P.K., Puusepp, L., Varghese, F.S., Utt, A., Ahola, T., Kananovich, D.G., Lopp, M., Merits, A., Karelson, M., 2016. Design and Validation of Novel Chikungunya Virus Protease Inhibitors. *Antimicrob Agents Chemother* 60, 7382-7395.
- De Clercq, E., Cools, M., Balzarini, J., Snoeck, R., Andrei, G., Hosoya, M., Shigeta, S., Ueda, T., Minakawa, N., Matsuda, A., 1991. Antiviral activities of 5-ethynyl-1-beta-D-ribofuranosylimidazole-4-carboxamide and related compounds. *Antimicrob Agents Chemother* 35, 679-684.
- De Clercq, E., Li, G., 2016. Approved Antiviral Drugs over the Past 50 Years. *Clin Microbiol Rev* 29, 695-747.
- Delang, L., Li, C., Tas, A., Querat, G., Albulescu, I.C., De Burghgraeve, T., Guerrero, N.A., Gigante, A., Piorkowski, G., Decroly, E., Jochmans, D., Canard, B., Snijder, E.J., Perez-Perez, M.J., van Hemert, M.J., Coutard, B., Leyssen, P., Neyts, J., 2016. The viral capping enzyme nsP1: a novel target for the inhibition of chikungunya virus infection. *Sci Rep* 6, 31819.
- Delang, L., Segura Guerrero, N., Tas, A., Querat, G., Pastorino, B., Froeyen, M., Dallmeier, K., Jochmans, D., Herdewijn, P., Bello, F., Snijder, E.J., de Lamballerie, X., Martina, B., Neyts, J., van Hemert, M.J., Leyssen, P., 2014. Mutations in the chikungunya virus non-structural proteins cause resistance to favipiravir (T-705), a broad-spectrum antiviral. *J Antimicrob Chemother* 69, 2770-2784.
- Eaton, H.E., Kobayashi, T., Dermody, T.S., Johnston, R.N., Jais, P.H., Shmulevitz, M., 2017. African Swine Fever Virus NP868R Capping Enzyme Promotes Reovirus Rescue during Reverse Genetics by

Promoting Reovirus Protein Expression, Virion Assembly, and RNA Incorporation into Infectious Virions. *J Virol* 91, e02416-02416.

Feibelman, K.M., Fuller, B.P., Li, L., LaBarbera, D.V., Geiss, B.J., 2018. Identification of small molecule inhibitors of the Chikungunya virus nsP1 RNA capping enzyme. *Antiviral Res* 154, 124-131.

Ferreira-Ramos, A.S., Li, C., Eydoux, C., Contreras, J.M., Morice, C., Querat, G., Gigante, A., Perez Perez, M.J., Jung, M.L., Canard, B., Guillemot, J.C., Decroly, E., Coutard, B., 2019. Approved drugs screening against the nsP1 capping enzyme of Venezuelan equine encephalitis virus using an immuno-based assay. *Antiviral Res* 163, 59-69.

Franco, E.J., Rodriguez, J.L., Pomeroy, J.J., Hanrahan, K.C., Brown, A.N., 2018. The effectiveness of antiviral agents with broad-spectrum activity against chikungunya virus varies between host cell lines. *Antivir Chem Chemother* 26, 2040206618807580.

Freund, I., Buhl, D.K., Boutin, S., Kotter, A., Pichot, F., Marchand, V., Vierbuchen, T., Heine, H., Motorin, Y., Helm, M., Dalpke, A.H., Eigenbrod, T., 2019. 2'-O-methylation within prokaryotic and eukaryotic tRNA inhibits innate immune activation by endosomal Toll-like receptors but does not affect recognition of whole organisms. *RNA* 25, 869-880.

Gigante, A., Canela, M.D., Delang, L., Priego, E.M., Camarasa, M.J., Querat, G., Neyts, J., Leyssen, P., Perez-Perez, M.J., 2014. Identification of [1,2,3]triazolo[4,5-d]pyrimidin-7(6H)-ones as novel inhibitors of Chikungunya virus replication. *J Med Chem* 57, 4000-4008.

Gomez-SanJuan, A., Gamo, A.M., Delang, L., Perez-Sanchez, A., Amrun, S.N., Abdelnabi, R., Jacobs, S., Priego, E.M., Camarasa, M.J., Jochmans, D., Leyssen, P., Ng, L.F.P., Querat, G., Neyts, J., Perez-Perez, M.J., 2018. Inhibition of the Replication of Different Strains of Chikungunya Virus by 3-Aryl-[1,2,3]triazolo[4,5-d]pyrimidin-7(6 H)-ones. *ACS Infect Dis* 4, 605-619.

Gullberg, R.C., Jordan Steel, J., Moon, S.L., Soltani, E., Geiss, B.J., 2015. Oxidative stress influences positive strand RNA virus genome synthesis and capping. *Virology* 475, 219-229.

Hardy, W.R., Strauss, J.H., 1989. Processing the nonstructural polyproteins of sindbis virus: nonstructural proteinase is in the C-terminal half of nsP2 and functions both in cis and in trans. *J Virol* 63, 4653-4664.

Horiuchi, K.Y., Eason, M.M., Ferry, J.J., Planck, J.L., Walsh, C.P., Smith, R.F., Howitz, K.T., Ma, H., 2013. Assay development for histone methyltransferases. *Assay Drug Dev Technol* 11, 227-236.

Hu, R.H., Lin, M.C., Hsu, Y.H., Meng, M., 2011. Mutational effects of the consensus aromatic residues in the mRNA capping domain of Bamboo mosaic virus on GTP methylation and virus accumulation. *Virology* 411, 15-24.

Hu, X., Compton, J.R., Leary, D.H., Olson, M.A., Lee, M.S., Cheung, J., Ye, W., Ferrer, M., Southall, N., Jadhav, A., Morazzani, E.M., Glass, P.J., Marugan, J., Legler, P.M., 2016. Kinetic, Mutational, and Structural Studies of the Venezuelan Equine Encephalitis Virus Nonstructural Protein 2 Cysteine Protease. *Biochemistry* 55, 3007-3019.

Huang, Y.L., Han, Y.T., Chang, Y.T., Hsu, Y.H., Meng, M., 2004. Critical residues for GTP methylation and formation of the covalent m7GMP-enzyme intermediate in the capping enzyme domain of bamboo mosaic virus. *J Virol* 78, 1271-1280.

Hyde, J.L., Gardner, C.L., Kimura, T., White, J.P., Liu, G., Trobaugh, D.W., Huang, C., Tonelli, M., Paessler, S., Takeda, K., Klimstra, W.B., Amarasinghe, G.K., Diamond, M.S., 2014. A viral RNA structural element alters host recognition of nonself RNA. *Science* 343, 783-787.

Kaur, R., Mudgal, R., Narwal, M., Tomar, S., 2018. Development of an ELISA assay for screening inhibitors against divalent metal ion dependent alphavirus capping enzyme. *Virus Res* 256, 209-218.

LaPointe, A.T., Moreno-Contreras, J., Sokoloski, K.J., 2018. Increasing the Capping Efficiency of the Sindbis Virus nsP1 Protein Negatively Affects Viral Infection. *MBio* 9, e02342-02318.

Law, Y.S., Utt, A., Tan, Y.B., Zheng, J., Wang, S., Chen, M.W., Griffin, P.R., Merits, A., Luo, D., 2019. Structural insights into RNA recognition by the Chikungunya virus nsP2 helicase. *Proc Natl Acad Sci U S A* 116, 9558-9567.

Lemm, J.A., Rumenapf, T., Strauss, E.G., Strauss, J.H., Rice, C.M., 1994. Polypeptide requirements for assembly of functional Sindbis virus replication complexes: a model for the temporal regulation of minus- and plus-strand RNA synthesis. *EMBO J* 13, 2925-2934.

Li, C., Guillen, J., Rabah, N., Blanjoie, A., Debart, F., Vasseur, J.J., Canard, B., Decroly, E., Coutard, B., 2015. mRNA Capping by Venezuelan Equine Encephalitis Virus nsP1: Functional Characterization and Implications for Antiviral Research. *J Virol* 89, 8292-8303.

Lin, H.Y., Yu, C.Y., Hsu, Y.H., Meng, M., 2012. Functional analysis of the conserved histidine residue of Bamboo mosaic virus capping enzyme in the activity for the formation of the covalent enzyme-m7GMP intermediate. *FEBS Lett* 586, 2326-2331.

Lwande, O.W., Obanda, V., Bucht, G., Mosomtai, G., Otieno, V., Ahlm, C., Evander, M., 2015. Global emergence of Alphaviruses that cause arthritis in humans. *Infect Ecol Epidemiol* 5, 29853.

Markland, W., McQuaid, T.J., Jain, J., Kwong, A.D., 2000. Broad-spectrum antiviral activity of the IMP dehydrogenase inhibitor VX-497: a comparison with ribavirin and demonstration of antiviral additivity with alpha interferon. *Antimicrob Agents Chemother* 44, 859-866.

Milhas, S., Raux, B., Betzi, S., Derviaux, C., Roche, P., Restouin, A., Basse, M.J., Rebuffet, E., Lugari, A., Badol, M., Kashyap, R., Lissitzky, J.C., Eydoux, C., Hamon, V., Gourdel, M.E., Combes, S., Zimmermann, P., Aurrand-Lions, M., Roux, T., Rogers, C., Muller, S., Knapp, S., Trinquet, E., Collette, Y., Guillemot, J.C., Morelli, X., 2016. Protein-Protein Interaction Inhibition (2P2I)-Oriented Chemical Library Accelerates Hit Discovery. *ACS Chem Biol* 11, 2140-2148.

Ogino, M., Ogino, T., 2017. 5'-Phospho-RNA Acceptor Specificity of GDP Polyribonucleotidyltransferase of Vesicular Stomatitis Virus in mRNA Capping. *J Virol* 91.

Pohjala, L., Barai, V., Azhaye, A., Lapinjoki, S., Ahola, T., 2008. A luciferase-based screening method for inhibitors of alphavirus replication applied to nucleoside analogues. *Antiviral Res* 78, 215-222.

Ravichandran, R., Manian, M., 2008. Ribavirin therapy for Chikungunya arthritis. *J Infect Dev Ctries* 2, 140-142.

Rikkinen, M., Peranen, J., Kaariainen, L., 1994. ATPase and GTPase activities associated with Semliki Forest virus nonstructural protein nsP2. *J Virol* 68, 5804-5810.

Rosenblum, C.I., Scheidel, L.M., Stollar, V., 1994. Mutations in the nsP1 coding sequence of Sindbis virus which restrict viral replication in secondary cultures of chick embryo fibroblasts prepared from aged primary cultures. *Virology* 198, 100-108.

Sales, G., Barbosa, I.C.P., Canejo Neta, L.M.S., Melo, P.L., Leitao, R.A., Melo, H.M.A., 2018. Treatment of chikungunya chronic arthritis: A systematic review. *Rev Assoc Med Bras (1992)* 64, 63-70.

Scheidel, L.M., Durbin, R.K., Stollar, V., 1987. Sindbis virus mutants resistant to mycophenolic acid and ribavirin. *Virology* 158, 1-7.

Scheidel, L.M., Stollar, V., 1991. Mutations that confer resistance to mycophenolic acid and ribavirin on Sindbis virus map to the nonstructural protein nsP1. *Virology* 181, 490-499.

Schulz, D., Rentmeister, A., 2012. An enzyme-coupled high-throughput assay for screening RNA methyltransferase activity in *E. coli* cell lysate. *RNA Biol* 9, 577-586.

Shirako, Y., Strauss, J.H., 1994. Regulation of Sindbis virus RNA replication: uncleaved P123 and nsP4 function in minus-strand RNA synthesis, whereas cleaved products from P123 are required for efficient plus-strand RNA synthesis. *J Virol* 68, 1874-1885.

Sokoloski, K.J., Haist, K.C., Morrison, T.E., Mukhopadhyay, S., Hardy, R.W., 2015. Noncapped Alphavirus Genomic RNAs and Their Role during Infection. *J Virol* 89, 6080-6092.

Stollar, V., Mensah, V., Adams, S., Li, M.L., 2013. Evolution of Sindbis virus with a low-methionine-resistant phenotype is dependent both on a pre-existing mutation and on the methionine concentration in the medium. *PLoS One* 8, e60504.

Tomar, S., Narwal, M., Harms, E., Smith, J.L., Kuhn, R.J., 2011. Heterologous production, purification and characterization of enzymatically active Sindbis virus nonstructural protein nsP1. *Protein Expr Purif* 79, 277-284.

Urakova, N., Kuznetsova, V., Crossman, D.K., Sokratian, A., Guthrie, D.B., Kolykhalov, A.A., Lockwood, M.A., Natchus, M.G., Crowley, M.R., Painter, G.R., Frolova, E.I., Frolov, I., 2017. beta-D-N(4)-hydroxycytidine is a potent anti-alphavirus compound that induces high level of mutations in viral genome. *J Virol* 92, e01965.

Vasiljeva, L., Merits, A., Auvinen, P., Kaariainen, L., 2000. Identification of a novel function of the alphavirus capping apparatus. RNA 5'-triphosphatase activity of Nsp2. *J Biol Chem* 275, 17281-17287.

Weaver, S.C., Winegar, R., Manger, I.D., Forrester, N.L., 2012. Alphaviruses: population genetics and determinants of emergence. *Antiviral Res* 94, 242-257.

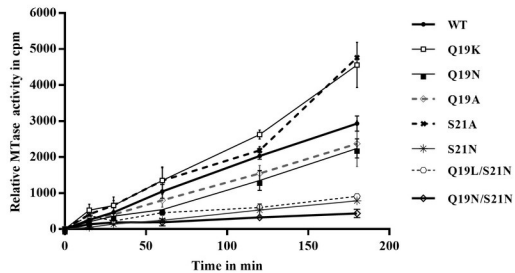
Zacks, M.A., Paessler, S., 2010. Encephalitic alphaviruses. *Vet Microbiol* 140, 281-286.

Zhao, B., Yi, G., Du, F., Chuang, Y.C., Vaughan, R.C., Sankaran, B., Kao, C.C., Li, P., 2017. Structure and function of the Zika virus full-length NS5 protein. *Nat Commun* 8, 14762.

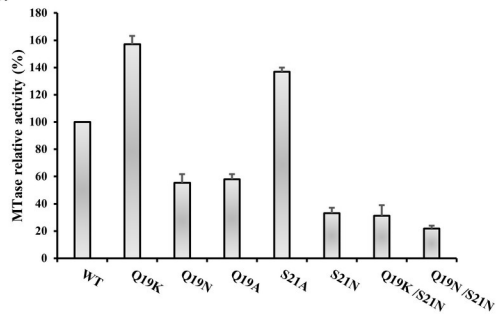
$\alpha 1$ $\beta 1$

1	10	20	30	39	301
VEEV	ME . K . . V H V D I E E D S P F L R A L	C R S	S F P Q F E V E A K Q V T D N D	H A N G L Y G K P S G Y A A T
SINV	ME . K P V V N V D V D P Q S P F V V Q L	C K S	S F P Q F E V V A Q Q V T P N D	H A N G I T G E T V G Y A V T
AURAV	ME . K P T V H V D V D P Q S P F V L Q L	C K S	S F P Q F E I V A Q Q V T P N D	H A N G I T G R V N R Y T V T
ONNV	MD . S . . V Y V D I D A D S A F L K A L	C Q A	Y P M F E V E P K Q V T P N D	H A N G I Y G K T S G Y A V T
CHIKV	MD . P . . V Y V D I D A D S A F L K A L	C R A	Y P M F E V E P R Q V T P N D	H A N G L Y G K T T G Y A V T
SFV	MAAK . . V H V D I E A D S P F I K S L	C K A	F P S F E V E S L Q V T P N D	H A N G L Y G K T V G Y A V T
MAYV	MS . K . . V F V D I E A E S P F L K S L	C R A	F P A F E V E A Q Q V T P N D	H A N G V F G K T S G Y A V T
BFV	MA . K P V V K I D V E P E S H F A K Q V	C S C	F P Q F E I E A V Q T T P N D	H A H G V T G K P I G Y A V T
EEEV	ME . K . . V H V D L D A D S P F V K S L	C R C	F P H F E I E A T Q V T D N D	H A N G I Y G K V D N L A S T
WEEV	ME . R . . I H V D L D A D S P Y V K S L	C R T	F P Q F E I E A R Q V T D N D	H A N G L Y G K V E N L A S T

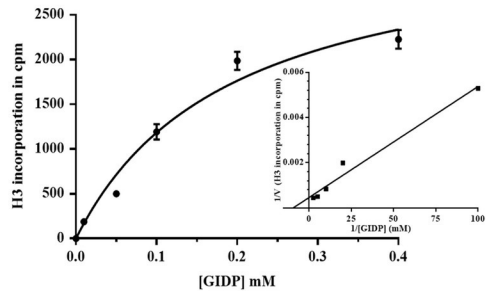
A.



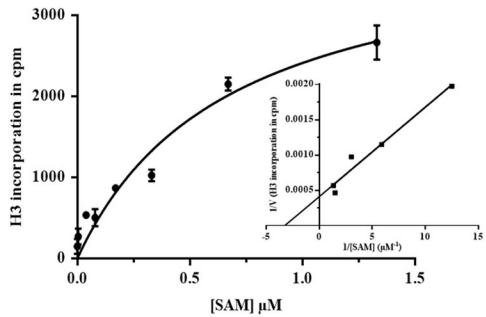
B.

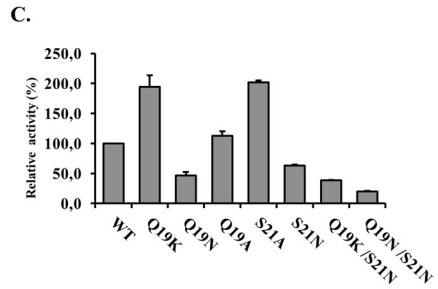
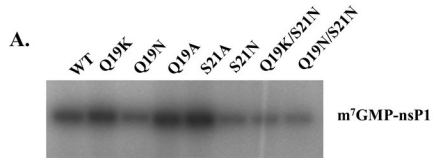


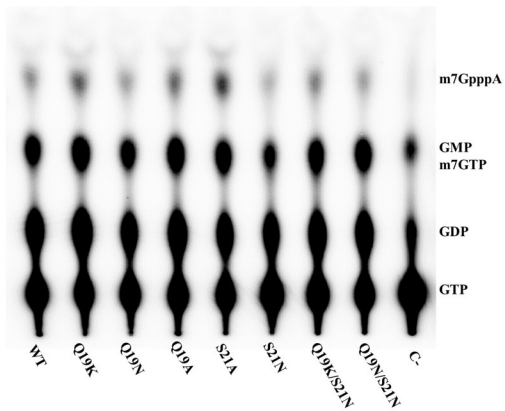
C.



D.





A.**B.**